




JULY 24 2023

Ventilated acoustic metasurface with low-frequency sound insulation

Yingxin Zhang; Yao Wei Chin; Xiang Yu; Milan Shrestha ; Gih-Keong Lau ; Boo Cheong Koo; Kun Liu; Zhenbo Lu 



JASA Express Lett. 3, 073602 (2023)

<https://doi.org/10.1121/10.0020133>



View
Online



Export
Citation

Articles You May Be Interested In

Membraned metasurface blocks noise but not air flow

Scilight (July 2023)

3D-printed sound absorber considering ventilation

JASA Express Lett. (December 2021)

Combined acoustic metamaterial design based on multi-channel Fano resonance effect

J. Appl. Phys. (July 2024)



ASA

Advance your science and career as a member of the
Acoustical Society of America

[LEARN MORE](#)

Ventilated acoustic metasurface with low-frequency sound insulation

Yingxin Zhang,^{1,a)} Yao Wei Chin,² Xiang Yu,³ Milan Shrestha,^{2,b)} Gih-Keong Lau,⁴ Boo Cheong Koo,² Kun Liu,^{1,a)} and Zhenbo Lu^{1,a),c)}

¹School of Aeronautics and Astronautics, Shenzhen Campus of Sun Yat-sen University, Shenzhen 518107, China

²Department of Mechanical Engineering, National University of Singapore, Singapore 117411, Singapore

³Department of Mechanical Engineering, The Hong Kong Polytechnic University, Hung Hom, Kowloon, Hong Kong Special Administrative Region

⁴Department of Mechanical Engineering, National Yang Ming Chiao Tung University, Hsinchu 30010, Taiwan

zhangyx289@mail2.sysu.edu.cn, yaowei_chin@nus.edu.sg, lucien.yu@polyu.edu.hk, MILAN001@e.ntu.edu.sg, mgklau@ncyu.edu.tw, mpekbc@nus.edu.sg, liukun6@mail.sysu.edu.cn, luzhb7@mail.sysu.edu.cn

Abstract: A ventilated acoustic metasurface consisting of a membrane covered with a combination of different depth sub-chambers is proposed. It can achieve at least a 5 dB sound insulation acoustic performance in the wide frequency range from 100 to 1700 Hz, in particular a 10 dB noise reduction in the range from 100 to 200 Hz and from 437.4 to 1700 Hz, which can therefore cover the low-frequency range of the environmental noise. The physical mechanism of membrane-acoustic coupling for noise reduction in the low-frequency range is further explored. © 2023 Author(s). All article content, except where otherwise noted, is licensed under a Creative Commons Attribution (CC BY) license (<http://creativecommons.org/licenses/by/4.0/>).

[Editor: Tracianne B. Neilsen]

<https://doi.org/10.1121/10.0020133>

Received: 3 May 2023 Accepted: 21 June 2023 Published Online: 24 July 2023

1. Introduction

Maintaining natural indoor ventilation while effectively insulating against external noise is a common requirement for urban residences and offices. However, achieving both of these goals simultaneously through a window is a challenging task. Conventional windows are designed to be opened for indoor-outdoor air circulation and closed for noise insulation. However, relying on only one of these features is not conducive to a comfortable indoor environment (Tang, 2017; Fusaro and Kang, 2021). Recently, researchers have developed various ventilated acoustic structures that can be used for noise insulation/reduction based on mechanical ventilation (Du *et al.*, 2020), perforated panels (Kang and Brocklesby, 2005), porous materials (Tsukamoto *et al.*, 2020), and hybrid passive/active control (ANC) systems (Kang and Brocklesby, 2005; Lam *et al.*, 2020a; Lam *et al.*, 2020b). However, structures incorporating passive methods such as plenum windows consisting of two staggered glass planes with two openings and porous materials are exceptionally thick or have less noticeable effects on long wavelength sound. The reliability of the ANC techniques cannot be guaranteed in practice due to the complexity of their composition (Pàmies *et al.*, 2014), and applying ANC systems to windows can compromise the sight and simplicity of appearance.

The development of acoustic metamaterials has enabled the achievement of exotic properties such as negative refraction (Xie *et al.*, 2013; Liu *et al.*, 2015), extraordinary transmission (Lu *et al.*, 2007; Zhou *et al.*, 2010; Park *et al.*, 2013), and wavefront modulation (Li *et al.*, 2014; Xie *et al.*, 2014), which were previously not possible with natural materials. Acoustic metasurfaces can achieve arbitrary modulation of the path of acoustic waves by the generalized Snell's law (Cummer *et al.*, 2016). Researchers have explored noise reduction with ventilation performances by employing various acoustic metamaterials such as ventilated subwavelength absorbers (Li *et al.*, 2018; Kumar *et al.*, 2020; Wang and Mao, 2021), sonic cages (Kumar *et al.*, 2022; Kumar and Lee, 2022), reconfigurable ventilation barriers (Chen *et al.*, 2021; Yin *et al.*, 2022; Xiao *et al.*, 2023), open metamaterial capable (Yu *et al.*, 2017; Wang *et al.*, 2019), and metawindows (Yu, 2019; Fusaro and Kang, 2021; Fusaro *et al.*, 2021). Although previous work has made great progress in acoustic metamaterials for noise control with natural ventilation, there are still limitations to overcome including the complex geometrical structure design, narrow bandwidth, and low-frequency effect. Therefore, designing a deep subwavelength silent ventilation window that can achieve broadband sound insulation covering low-frequency range noise with a compact structure remains a great challenge. Membrane-type acoustic metamaterials have the advantage of being lightweight and compact

^{a)}Also at: School of Aeronautics and Astronautics, Sun Yat-sen University, Shenzhen 518107, China.

^{b)}Also at: Continental-NTU Corporate Lab, Nanyang Technological University, Singapore 639798.

^{c)}Author to whom correspondence should be addressed.

and allowing for near-total reflection at certain low-frequency ranges (Yang *et al.*, 2008). Studies utilizing thin membranes have been shown to achieve broadband effective acoustic insulation at low-frequency range (Lu *et al.*, 2020; Sampaio *et al.*, 2022). However, little work has been done with such a membrane-type design to develop a fully natural ventilation window for noise insulation.

2. Ventilated acoustic metasurface

An acoustic ventilated metasurface consisting of an elastic membrane covered and fixed by a combination of sub-chambers with varying depths (as shown in Fig. 1) is proposed for a silent ventilation window design, which can satisfy both natural ventilation and noise isolation. It provides broadband sound insulation in the extreme low-frequency range, which is extremely challenging, and a central opening on the structure can provide a path for indoor-outdoor natural air circulation. The structure-acoustic coupling mechanism between the membrane and back sub-chambers with varying depths is the key physical factor for such a design. As shown in Fig. 1, the side covered with the membrane of the metasurface is placed facing the outdoor environment while the other side with only the rigid surface faces the indoor environment. When the outdoor environment noise propagates through the VAM, the acoustic-membrane coupling between the soft surface and the air inside the sub-chamber will alter the propagation direction of the sound waves, and then the noise is propagated back to the outdoor environment. Therefore, as shown in Fig. 1(c), the sound entering from the central vent propagates along the sub-chambers and diffuses back to the noise source side without continuing to go through the VAM to the interior via the sub-chamber scattering and the acoustic-membrane interactions.

The VAM unit consists of a symmetrical cube with a three-dimensional dimension of 244 mm × 244 mm × 93 mm and a square vent of 60 mm × 60 mm in the center of the structure, with opening and open ratios of 3600 mm² and 6.25%, respectively. The overall thickness of the whole unit is less than 100 mm. The back chamber consists of resonant sub-chambers with varying depths: 240, 200, 176, 150, and 240 mm, each with a thickness of 15 mm and a 2 mm acrylic plate between the sub-chambers and front and rear frameworks of 5 mm. These metasurface units of the ventilation acoustic window are assembled in arrays for achieving a broader noise insulation band.

3. Numerical modelling and experimental configuration

Since there are only limited studies on the use of a membrane in the design of VAM, it is crucial to describe the impact of membrane-acoustic coupling on the design and to develop precise numerical modelling to calculate the composite. The acoustic performance of the VAM is first assessed using a finite element multiphysical interaction model for membrane-acoustic coupling and then verified by an acoustic duct measurement system. Multiphysics commercial software COMSOL

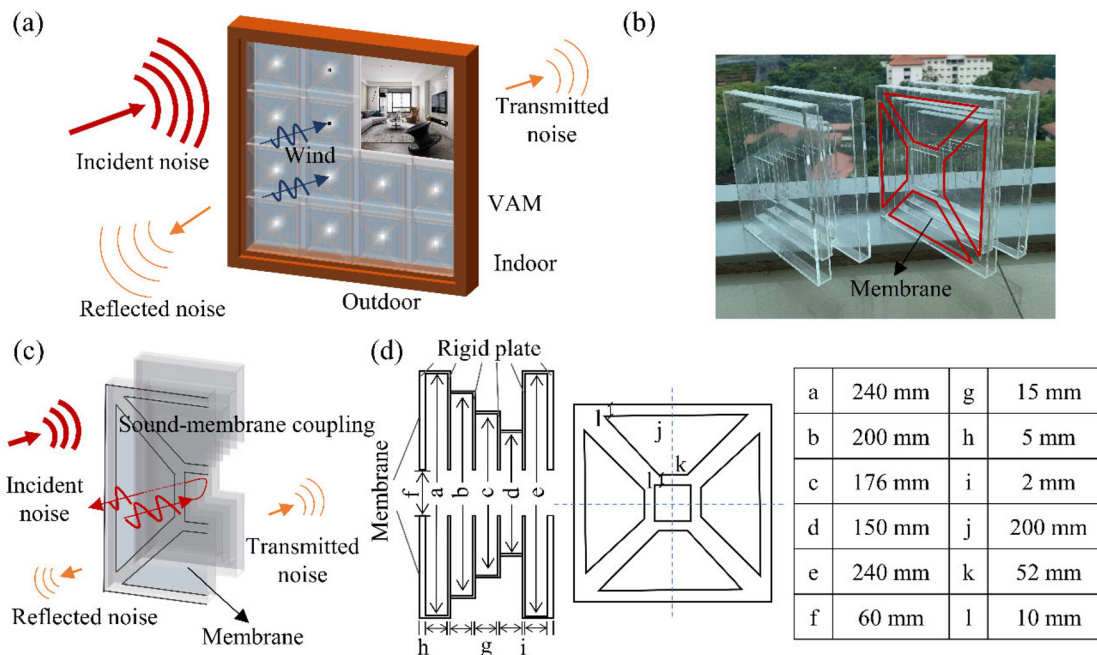


Fig. 1. A ventilated acoustic metasurface (VAM) with membrane: (a) diagram of a silent ventilation window made of an array of acoustic metasurfaces; (b) the photograph of VAM; (c) VAM unit membrane- acoustic coupling principle; (d) VAM consists of sub-chambers with various depths.

was used for developing the finite element model. Figure 2(a) shows the schematics of the VAM unit configuration. Using the ventilated acoustic metasurface unit shown in Fig. 1, the side covered by a membrane faces the noise source. In this way, it can diffuse back part of the noise via the membrane-acoustic coupling mechanism. A surface source is used to produce plane acoustic waves and applied to the 60 mm × 60 mm duct left boundary. The upper and lower sections of the VAM are set to be the air domain surrounded on four sides of the duct and perfectly matched layers (PMLs) are used at each end of the duct and wrapped air domain to guarantee the non-reflection condition, which means the sound propagates through the duct exits without the reflected waves.

The numerical model is developed based on a pressure acoustics field, considering the contribution of membrane vibrations to the acoustic performance of the proposed VAM unit, simulating the elastic membrane (FUNCTECH XGT0158, Polyester TPU film) in the structural mechanic's field as a membrane with a thickness of 0.1 mm. When no thin membrane is present, the model can simulate completely using only pressure acoustics. The walls of the VAM are assumed to be rigid and can be described using sound hard boundary conditions. The sound hard boundary (wall) adds a boundary condition for a sound hard boundary or wall, which is a boundary at which the normal component of the acceleration (and thus the velocity) is zero,

$$-\mathbf{n} \cdot (-\nabla p_t - \mathbf{q}_d) / \rho_c = 0, \tag{1}$$

where \mathbf{n} is the normal direction of the membrane surface, p_t is the total sound pressure, \mathbf{q}_d dipole domain source and, ρ_c is the air density.

Due to the presence of the membrane, the finite element model should be established to predict the wave behavior by the air and membrane parts, considering the membrane and the quarter-wave type sub-chambers will be coupled between the different media; it is important to capture what happens at the air-membrane interfacing boundaries. To solve these problems and complete an accurate numerical model, the acoustic-structural boundary has to be used to describe the membrane-acoustic interaction generated after taking the membrane into account. The feature applies continuity of the air pressure on the boundaries which includes two parts: a boundary load from the air pressure on the elastic waves in the membrane and the normal acceleration of the membrane experienced by the air. The boundary conditions can be formulated by the following equations:

$$-\mathbf{n} \cdot (-\nabla p_t - \mathbf{q}_d) / \rho_c \Big|_{\text{up}} = -\mathbf{n} \cdot \mathbf{u}_{tt}, \tag{2}$$

$$-\mathbf{n} \cdot (-\nabla p_t - \mathbf{q}_d) / \rho_c \Big|_{\text{down}} = -\mathbf{n} \cdot \mathbf{u}_{tt}, \tag{3}$$

$$\mathbf{F}_A = (p_{t,\text{down}} - p_{t,\text{up}}) \mathbf{n}, \tag{4}$$

where \mathbf{u}_{tt} is the acceleration of the membrane and \mathbf{F}_A is the force load per unit area acting on the membrane. The “up” and “down” subscripts refer to two sides of the membrane, so that the acoustic load is described by the pressure drop on both sides of the membrane to realize the establishment of the direct coupling and interaction model of the membrane-acoustic structure.

An experimental setup for measuring transmission loss of VAM is shown in Fig. 2(b) The acoustic experimental setup is mainly composed of a duct with a square cross section of side length 100 mm. A loudspeaker (BMS, 12CN860) is installed on one side of the duct as a sound source. Four microphones (PCB, 130F20) marked as “Mic1,” “Mic2,” “Mic3,” and “Mic4,” respectively, are used to measure the sound pressure inside the duct. Hence, Mic1 and Mic2 are placed 30 mm away from each other, which is the same distance for Mic3 and Mic4. Mic1 is regarded as the reference microphone of the setup and is used to calibrate the amplitude and phase of the other three microphones. The measured sound pressure is calculated to construct the matrix parameters of the transfer matrix measurement method (Munjal and Doige,

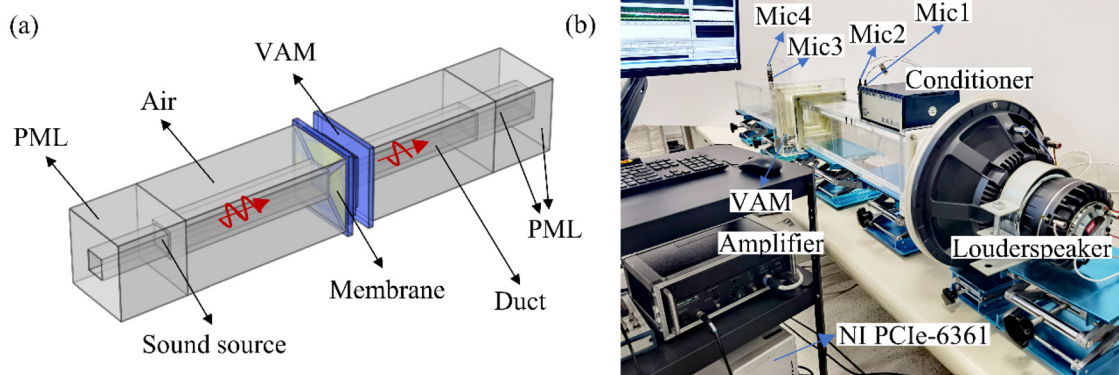


Fig. 2. Numerical and experimental setup (a) VAM configuration in the COMSOL and (b) acoustic duct system.

1990), and the advantage of this approach for measurement is a high measurement accuracy with a simple structure; this means an anechoic end can be absent in the acoustic system. The VAM unit is placed in the middle of the measurement system, and the rectangular duct is connected to the 60 mm × 60 mm VAM vent through two transition sections. The membrane is placed on the side facing the loudspeaker to be like VAM’s actual use on a window. The measurement frequency range of the current system is from 100 Hz to 1700 Hz. In addition, all acquisition and control signals are conducted by NI PCI-6251 with a sampling rate of 40 kHz.

4. Results and discussions

The acoustic performance of the silent ventilation window unit without incorporating the membrane design is separately verified by simulation and experiment. Its back chamber structure is illustrated in Fig. 1(c). With the exception of the absence of the membrane, all the settings are consistent with the membrane-based VAM unit proposed in this letter. The sound transmission loss results of the VAM are shown in Fig. 3(a), to facilitate a view of the results in the low-frequency range. In particular, the regime below 500 Hz in the upper part of Fig. 3(a) is enlarged to the lower one. The silent ventilation structure composed of varying depth sub-chambers only has a wide frequency noise insulation band in the middle-frequency and high-frequency ranges, and the numerical and experimental results are well fitted, both showing an effective reduction of 10 dB in the range of 500–1700 Hz can be achieved. However, the structure is still not sufficient for sound insulation below 500 Hz, which can only achieve an approximate value of 5 dB reduction.

Observing the acoustic performance of the VAM proposed in the current work, as shown in Fig. 3(a), the results of simulation and experimental have agreed rather well, especially in the low-frequency range where the two distributions nearly overlap. It is shown that the membrane-acoustic coupling simulation model used in this letter can produce the experiment to a high degree. As such, the high fidelity and reliability of the simulation model can be used to further reveal the mechanism of the VAM which has produced better acoustic performance. The noise stop band of VAM after the applying membrane can cover 100–1700 Hz with a 5 dB noise reduction effect in the needed range. It is noteworthy that the noise reduction of 10 dB in the 100–200 Hz and 437.4–1700 Hz ranges almost covers the frequency range of various typical noises. Thin membranes have a lower elastic modulus than plate materials and can generate vibrational eigenmodes at low frequencies. The proposed VAM with excellent sound insulation properties is a natural consequence of the presence of multiple low-frequency eigenmodes in the system. Thus, the proposed thin-membrane acoustic metamaterials greatly improve the sound insulation effect in the low-frequency range.

Figures 3(b) and 3(c) show the sound pressure distributions and highlight the interesting coherence between the membrane-acoustic coupling and the sound pressure distribution around the membrane. There is a variation in sound pressure inside the duct and the metasurface unit, and the sound pressure in the whole surrounding air domain is zero.

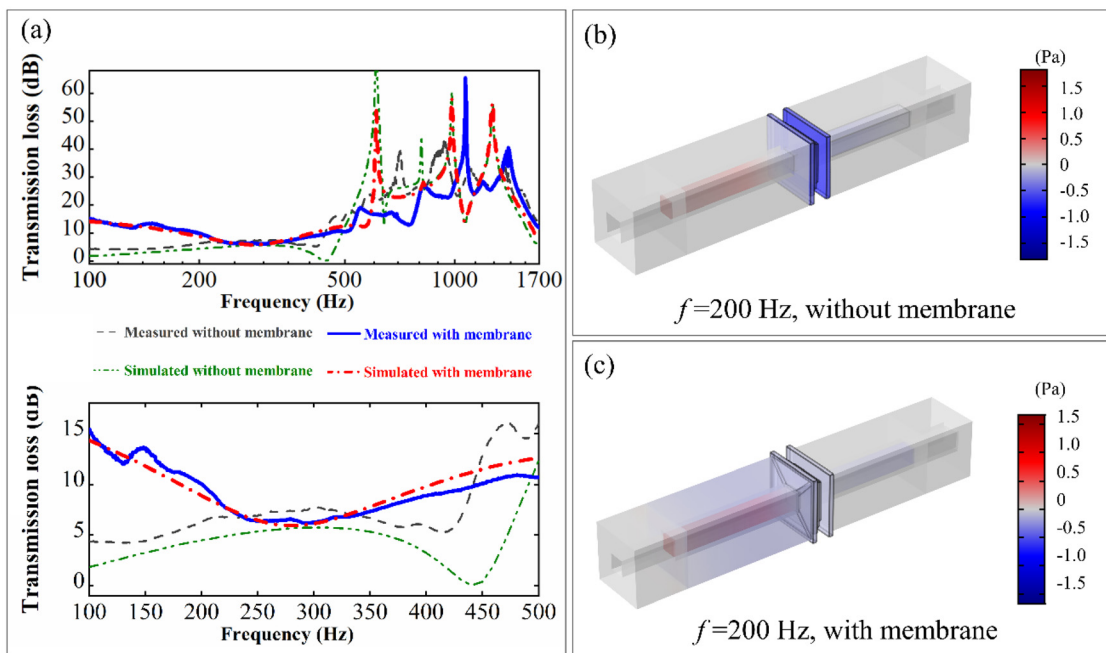


Fig. 3. (a) Comparison of transmission loss related to the numerical and experimental results on VAM unit with a membrane covering and VAM unit with sub-chambers only. Sound pressure distribution in the VAM at 200 Hz: (b) sound pressure without membrane; (c) sound pressure with membrane.

When a thin membrane is added, the variation in sound pressure in the simulation extends from the duct to the air domain upstream of the VAM. The noticeable expansion of the range of sound pressure fluctuations indicates that the sound essentially propagates only in the duct without the membrane. It changes to transmit the vibration to the air on the side of the membrane with the addition of the membrane, and the range of air for resonance increases obviously. In turn, it is found that without a membrane, when sound propagates from the duct to the metasurface unit, only the sub-chamber scattering mechanism is advised inside the metasurface to achieve noise insulation. After the membrane is added, the VAM facing the sound source receives the acoustic excitation and the acoustic-membrane interaction between the membrane and the air inside the VAM sub-chamber is triggered. As shown in Fig. 3(c), the sound entering from the central vent then propagates along the sub-chamber and then diffuses back to the incident side through the membrane, so that the sound energy is reflected upstream without continuing to propagate through the VAM to the downstream.

5. Membrane-acoustic coupling mechanism

To investigate how the incorporation of the membrane induces a better acoustic performance in the low-frequency range of the silent ventilation window, the simulation results in the numerical models are further analyzed. First, the pressure isosurface inside the VAM structure in the low-frequency range is shown in Figs. 4(a) and 4(b). It can be observed that if no membrane is added, the isobaric surface is distributed in a circular-like column at the center of the ventilation aperture, with a symmetrical curved distribution at the corners. This pattern is due to the coupling between sub-chambers with various depths, which leads to the wide stop band noise insulation effect. With the addition of the membrane, the pattern of the isobaric surface changes significantly, with the shape of the central isobaric column assuming a petal shape and the form at the four corners keeping to a symmetrical curved distribution with bending curvature. This is the effect of the membrane coupling with the sound as it enters through the central vent and the membrane coupling with the air inside the VAM at the central vent so that the noise enters from the vent and diffuses back to the incoming side. Thus, the complex isobaric surface distribution of the membrane, as the surface on the side of the proposed VAM, is varied as shown.

Further, the incorporation of the membrane causes the transfer of relevant physical quantities between the resonances in sub-chambers of the VAM and the membrane during the motion, mainly in terms of vibration resulting in a velocity transfer. Several typical resonance frequencies in the low-frequency range were selected to observe the vibration modes of the membrane, as shown in Figs. 4(c) and 4(d). The membranes show significantly different velocity distributions at different frequency ranges, thereby indicating that the vibration pattern of the membrane changes corresponding to different excitation frequencies. At the same time, the vibration of the membrane is quarter-symmetrically distributed at all four frequency distributions mentioned above, which is consistent with the setup where the four membranes covering

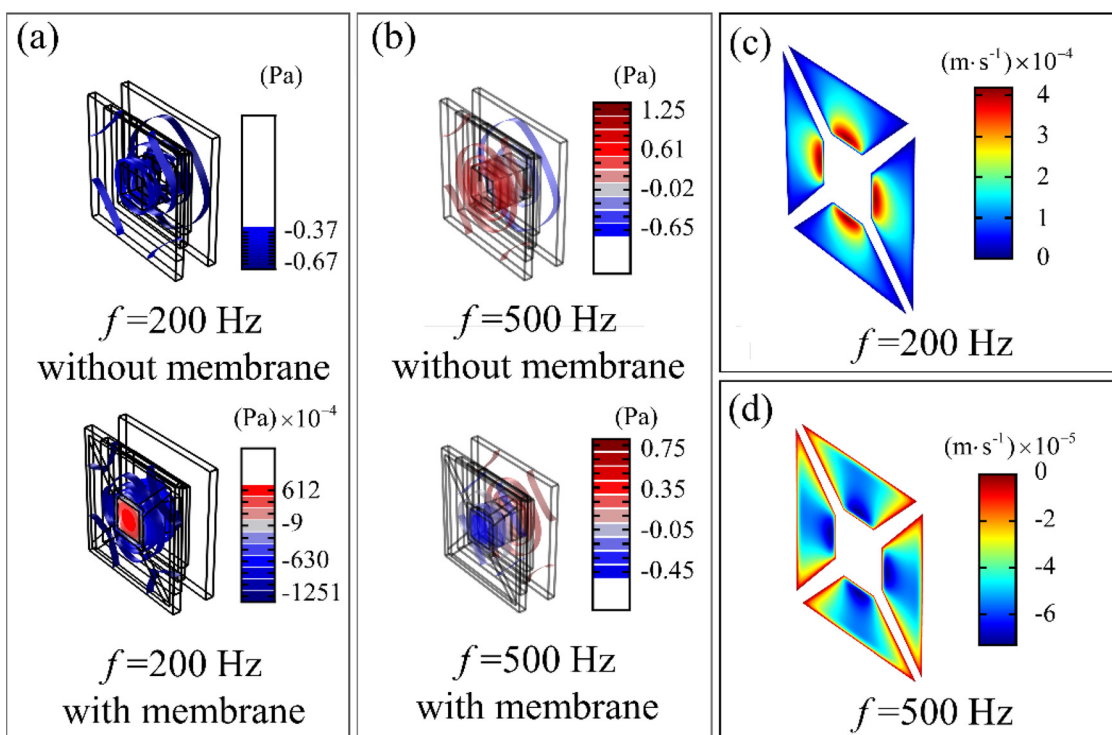


Fig. 4. Comparison of pressure isosurface inside VAM unit with and without membrane (a) at 200 Hz and (b) at 500 Hz. Distribution of vibration velocities of (c) $f=100$ Hz and (d) $f=500$ Hz membranes at different frequencies.

the VAM back cavity are symmetrically distributed. The four sides of each trapezoidal membrane are fixed and the vibration velocity at the solid fixed support boundary is zero. As such, the vibration velocity amplitude near the central vent is larger and the vibration intensity is high. The use of a thin membrane for VAM allows the silent ventilation structure to acquire additional new vibrational modes, especially in the low-frequency range to generate more resonance peaks, thus enhancing the acoustic performance of VAM at low frequencies. This corresponds to the aforementioned mechanism revealed by the pressure isosurface inside the VAM unit, whereby sound enters the VAM unit through the vent, and sound energy is diffused back into the incident side by the membrane and coupling.

6. Conclusion

In summary, we have proposed a silent ventilation metasurface that has broad stopbands and low-frequency sound insulation. It consists of a back cavity of various depths, a central vent, and thin membranes on one side. A minimum 5 dB broadband noise insulation band in the range of 100–1700 Hz is achieved with a 10 dB broadband noise insulation stop band covering most frequencies in this range. The VAM is particularly effective for low-frequency noise (100–200 Hz) which is a great challenge for noise control problems. Incident noise impacting the membrane triggers an acoustic-structural coupling between the membrane and the air in the VAM sub-chambers. The noise entering from the central vent then propagates along the sub-chamber and is retransmitted back to the incident sound side by vibrational reflection from the membrane, thus providing sound insulation in the low-frequency range. The various depths of the sub-chambers are coupled to each other, which provides a broad frequency noise reduction stop band. This metasurface, which is a compact structure, has great potential for achieving interior silent ventilation windows, especially effective in low-frequency and broadband sound insulation.

Acknowledgments

This study was supported by the Shenzhen Science and Technology Program (Grant Nos. GXWD20201231165807008, 20200830220051001), the National Natural Science Foundation of China (Grant No. 52250217), Shenzhen Science and Technology Program (Grant No. JCYJ20220530145205013), the Department of Science and Technology of Guangdong Province (Grant No. 2019QN01G064), Temasek Foundation Innovates and Temasek Foundation Ecosperity.

References and links

- Chen, D.-C., Wei, Q., Yan, P., Zhu, X., and Wu, D. (2021). "Sound insulation via a reconfigurable ventilation barrier with ultra-thin zigzag structures," *J. Appl. Phys.* **129**, 064502.
- Cummer, S. A., Christensen, J., and Alú, A. (2016). "Controlling sound with acoustic metamaterials," *Nat. Rev. Mater.* **1**, 16001.
- Du, L., Lau, S.-K., Lee, S. E., and Danzer, M. K. (2020). "Experimental study on noise reduction and ventilation performances of sound-proofed ventilation window," *Build. Environ.* **181**, 107105.
- Fusaro, G., and Kang, J. (2021). "Participatory approach to draw ergonomic criteria for window design," *Int. J. Ind. Ergonom.* **82**, 103098.
- Fusaro, G., Yu, X., Lu, Z., Cui, F., and Kang, J. (2021). "A metawindow with optimised acoustic and ventilation performance," *Appl. Sci.* **11**, 3168.
- Kang, J., and Brocklesby, M. W. (2005). "Feasibility of applying micro-perforated absorbers in acoustic window systems," *Appl. Acoust.* **66**, 669–689.
- Kumar, S., Aow, J. W., and Lee, H. P. (2022). "Acoustical performance of ventilated aluminum T-slot columns-based sonic cage," *Appl. Acoust.* **193**, 108779.
- Kumar, S., and Lee, H. P. (2022). "Acoustic performance of sonic metacage consisting of Helmholtz's resonator columns with internal partitions," *Appl. Acoust.* **196**, 108887.
- Kumar, S., Xiang, T. B., and Lee, H. P. (2020). "Ventilated acoustic metamaterial window panels for simultaneous noise shielding and air circulation," *Appl. Acoust.* **159**, 107088.
- Lam, B., Shi, D., Belyi, V., Wen, S., Gan, W.-S., Li, K., and Lee, I. (2020a). "Active control of low-frequency noise through a single top-hung window in a full-sized room," *Appl. Sci.* **10**, 6817.
- Lam, B., Shi, D., Gan, W.-S., Elliott, S. J., and Nishimura, M. (2020b). "Active control of broadband sound through the open aperture of a full-sized domestic window," *Sci. Rep.* **10**, 10021.
- Li, L., Zheng, B., Zhong, L., Yang, J., Liang, B., and Cheng, J. (2018). "Broadband compact acoustic absorber with high-efficiency ventilation performance," *Appl. Phys. Lett.* **113**, 103501.
- Li, Y., Jiang, X., Li, R., Liang, B., Zou, X., Yin, L., and Cheng, J. (2014). "Experimental realization of full control of reflected waves with subwavelength acoustic metasurfaces," *Phys. Rev. Appl.* **2**, 064002.
- Liu, J., Hou, Z., and Fu, X. (2015). "Negative refraction realized by band folding effect in resonator-based acoustic metamaterials," *Phys. Lett. A* **379**, 2097–2101.
- Lu, M., Liu, X., Feng, L., Li, J., Huang, C., Chen, Y., Zhu, Y., Zhu, S., and Ming, N. (2007). "Extraordinary acoustic transmission through a 1D grating with very narrow apertures," *Phys. Rev. Lett.* **99**, 174301.
- Lu, Z., Yu, X., Lau, S.-K., Khoo, B. C., and Cui, F. (2020). "Membrane-type acoustic metamaterial with eccentric masses for broadband sound isolation," *Appl. Acoust.* **157**, 107003.
- Munjal, M. L., and Doige, A. G. (1990). "Theory of a two source-location method for direct experimental evaluation of the four-pole parameters of an aeroacoustic element," *J. Sound Vib.* **141**, 323–333.
- Pàmies, T., Romeu, J., Genescà, M., and Arcos, R. (2014). "Active control of aircraft fly-over sound transmission through an open window," *Appl. Acoust.* **84**, 116–121.

- Park, J. J., Lee, K. J. B., Wright, O. B., Jung, M. K., and Lee, S. H. (2013). "Giant acoustic concentration by extraordinary transmission in zero-mass metamaterials," *Phys. Rev. Lett.* **110**, 244302.
- Sampaio, L. Y. M., Cerântola, P. C. M., and de Oliveira, L. P. R. (2022). "Lightweight decorated membranes as an aesthetic solution for sound insulation panels," *J. Sound Vib.* **532**, 116971.
- Tang, S.-K. (2017). "A review on natural ventilation-enabling façade noise control devices for congested high-rise cities," *Appl. Sci.* **7**, 175.
- Tsakamoto, Y., Tomikawa, Y., Sakagami, K., Okuzono, T., Maikawa, H., and Komoto, Y. (2020). "Experimental assessment of sound insulation performance of a double window with porous absorbent materials its cavity perimeter," *Appl. Acoust.* **165**, 107317.
- Wang, H., and Mao, Q. (2021). "Development and investigation of fully ventilated deep subwavelength absorbers," *Symmetry* **13**, 1835.
- Wang, X., Luo, X., Yang, B., and Huang, Z. (2019). "Ultrathin and durable open metamaterials for simultaneous ventilation and sound reduction," *Appl. Phys. Lett.* **115**, 171902.
- Xiao, Z., Gao, P., He, X., Qu, Y., and Wu, L. (2023). "Multifunctional acoustic metamaterial for air ventilation, broadband sound insulation and switchable transmission," *J. Phys. D: Appl. Phys.* **56**, 044006.
- Xie, Y., Popa, B.-I., Zigoneanu, L., and Cummer, S. A. (2013). "Measurement of a broadband negative index with space-coiling acoustic metamaterials," *Phys. Rev. Lett.* **110**, 175501.
- Xie, Y., Wang, W., Chen, H., Konneker, A., Popa, B.-I., and Cummer, S. A. (2014). "Wavefront modulation and subwavelength diffractive acoustics with an acoustic metasurface," *Nat. Commun.* **5**, 5553.
- Yang, Z., Mei, J., Yang, M., Chan, N. H., and Sheng, P. (2008). "Membrane-type acoustic metamaterial with negative dynamic mass," *Phys. Rev. Lett.* **101**, 204301.
- Yin, Y., Wu, H., Cheng, S., Sun, W., and Sheng, Z. (2022). "Acoustic metacage with arbitrary shape for broadband and ventilated sound insulation," *J. Appl. Phys.* **132**, 145101.
- Yu, X. (2019). "Design and in-situ measurement of the acoustic performance of a metasurface ventilation window," *Appl. Acoust.* **152**, 127–132.
- Yu, X., Lu, Z., Cheng, L., and Cui, F. (2017). "On the sound insulation of acoustic metasurface using a sub-structuring approach," *J. Sound Vib.* **401**, 190–203.
- Zhou, Y., Lu, M., Feng, L., Ni, X., Chen, Y., Zhu, Y., Zhu, S., and Ming, N. (2010). "Acoustic surface evanescent wave and its dominant contribution to extraordinary acoustic transmission and collimation of sound," *Phys. Rev. Lett.* **104**, 164301.